

Magnetic Structures and Pressure Profiles in the Plasma Boundary of RFX-mod: High Current and Density Limit in Helical Regimes

P. Scarin, N. Vianello, M. Agostini, S. Cappello, L. Carraro, R. Cavazzana, G. De Masi, E. Martines, M. Moresco, S. Munaretto, M. E. Puiatti, G. Spizzo, M. Spolaore, M. Valisa, M. Zuin and the RFX-mod team

Consorzio RFX, Associazione EURATOM-ENEA sulla fusione, Padova, Italy

e-mail contact of main author: paolo.scarin@igi.cnr.it

Abstract. New edge diagnostics and detailed analysis of the magnetic topology have significantly improved the comprehension of the processes developing at the boundary of the Reversed Field Pinch (RFP) plasma in RFX-mod ($a=0.46\text{m}$, $R=2\text{m}$).

An upper critical density $n_C \approx 0.4n_G$ (n_G Greenwald density) is found to limit the operational space for the improved Quasi Single Helical (QSH) regime: magnetic topology reconstructions and diagnostic observations suggest that this limit is due to a helical plasma wall interaction (PWI) which determines toroidally and poloidally localized edge density accumulation and cooling.

The experimental evidence is provided by a variety of diagnostics: the magnetic boundary as reconstructed from equilibrium codes reveal a helical deformation, which is well correlated with the modulation of edge pressure profile as reconstructed from the Thermal Helium Beam diagnostic and with edge density as estimated from the microwave reflectometer. Correlations with the helical deformation are also observed on the space and time resolved pattern of the floating potential measured at the wall, and with the toroidal plasma flow in the edge obtained from different diagnostics: Gas Puffing Imaging (GPI) system, Gundestrup probe and Internal System of Sensor (ISIS). All of these observations suggest that the QSH persistence is limited by processes originating in the plasma boundary.

1. Introduction

The Reversed-Field Pinch (RFP) RFX-mod ($a=0.46\text{m}$, $R=2\text{m}$) exploits a toroidal configuration for plasma confinement with the safety factor profile q monotonically decreasing from the core to the edge, where it changes sign. The $q=0$ surface, called reversal surface, is characterized by rather peculiar transport properties: it has been shown that this surface hosts a chain of islands with their O and X-points aligned in the toroidal direction, which, according to numerical simulations, reduces ion transport in the plasma boundary [1]. The amelioration of the plasma boundary control through the feedback system of active coils [2] and the increase of plasma current induced the development of dynamical helical regimes (Quasi Single Helical topology: QSH states). These states show a peaked MHD spectrum with a dominant mode $m=1$, $n=-7$, different from the flat spectrum of the Multiple Helicity (MH) state. The QSH exhibits good magnetic flux surfaces with an electron internal transport barrier [3], instead of magnetic chaos and flat pressure profiles which are found in MH. The QSH states are characterized by a persistence of the dominant mode that undergoes fast interruptions (crashes), linked to magnetic reconnection events [3].

The purpose of this paper is to show that the helical topology, typical of the QSH plasma core, deeply influences also the boundary. The helical deformation induced by the dominant mode is found to modulate the edge electron pressure profile, as shown by the Thermal Helium Beam (THB) diagnostic [4] (which measures the electron density and temperature from the line intensities ratio of HeI lines). The floating potential V_f , as obtained from the Integrated System of Internal Sensor (ISIS) [5], is also found to be correlated with the helical shift as reconstructed from the edge magnetic measurements [6]. Presently the QSH is found to depend on plasma equilibrium and consequently on the value of the edge q , $q(a)$ [7]. The second issue of this paper regards QSH dynamics, namely to study the transition from QSH to

MH states (and backwards from MH to QSH) as a function of the normalized plasma density n/n_G , and to show that this transition is deeply influenced by the boundary conditions.

In the analysis a central role is assumed by the edge radial electric field $E_r \approx v_\phi \cdot B_\theta$, which is deduced from the experimental measurements of the toroidal flow v_ϕ , neglecting the diamagnetic contribution [8]. A simplified analytical calculation of E_r can be obtained considering the electron and ion perpendicular diffusion in a sheath next to the wall: the result is an ambipolar field [9] which tends to balance the fluxes of the two species. This ambipolar field is toroidally modulated by the presence of a chain of $(m=0, n=7)$ islands aligned along the reversal surface [10]. According to numerical simulations, the ion diffusion is found to be

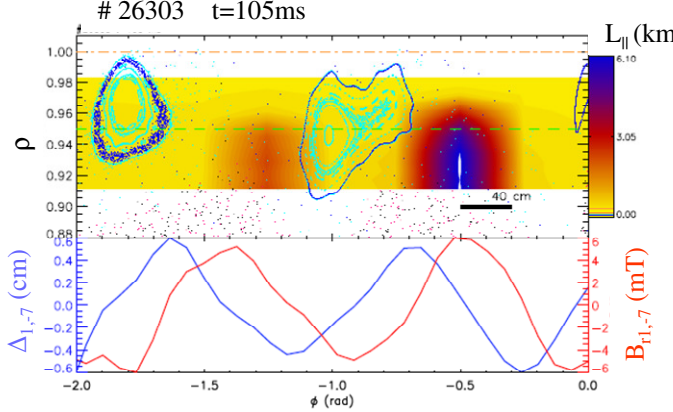


Fig.1: (up) Edge Poincaré plot ($\theta=0^\circ$) of $(0,7)$ island chain and characteristic electron length $L_{||}$ (color contour map); (down) toroidal behavior of the shift of dominant mode $\Delta_{1,-7}$ (blue) and of corresponding radial magnetic field (red).

similar in O and X-points of the $(0,7)$ islands, whereas electrons spend more time in X-points due to their smaller drifts. Consequently, X-points present a relative higher electron concentration: the result is a toroidal modulation of electron diffusion. The same modulation is observed also in the electron pressure P_e , in the floating potential V_f and H_α emission: all of these quantities are found to be intimately related to the plasma shift induced by the dominant mode $\Delta_{1,-7}$, and to the radial magnetic perturbation $B_{r1,-7}$.

The paper is organized as follows:

a description of the plasma boundary is provided in section 2 that gives a picture of the link between the magnetic and kinetic measurements. In section 3 the QSH persistence is considered and the link with the magnetic reconnections is presented. In section 4 the comparison between the particles in-flux from H_α measurements and out-flux from intermittent events at different magnetic shift is shown. In section 5 the discussion about the QSH density limit is introduced and finally in section 6 we draw our conclusions.

2. Plasma Boundary: description of the static spatial patterns

2.1 Magnetic structure reconstruction

The edge region of RFX-mod in QSH regimes is characterized by the presence of a chain of $(0,7)$ islands arising as an effect of toroidicity and mode coupling [1, 10]. The radial width of the islands, $5 \div 7$ cm, is comparable with those characterizing the MH states [9]. The main difference between QSH and MH in the edge topology is the absence in QSH of the $(m=0, n=1)$ mode, which in MH introduces a strong toroidal asymmetry. In QSH instead the chain of islands is uniform, with the X- and O-points aligned along the reversal surface. In Fig.1 a Poincaré plot at poloidal angle $\theta=0^\circ$ (top panel) obtained with the guiding centre code Orbit [11] is shown, where the $(0,7)$ islands are highlighted together with the contour map of the parallel electron characteristic length $L_{||}(r, \phi)$. The latter represents the length of the electron path to the wall (parallel to the magnetic field) from their initial position $\rho=0.9, \theta=0^\circ, \phi$ uniform. This length is found to exhibit a modulation due to the presence of the X-points characterized by values more than one order of magnitude higher than those found in O-

points. In the bottom panel of Fig.1 the shift of the dominant mode $\Delta_{1,-7}(\phi)$ and the corresponding radial magnetic field $B_{r1,-7}(\phi)$ are also shown as a function of the toroidal angle ϕ for a fixed time. The maximum of the radial shift is between the O- and X-points of the islands, whereas the maximum radial magnetic field corresponds to the X-points, due to the phase relation between the $(m=1, n=-7)$ mode and its $m=0$ counterpart. As far as particle source and diffusion are concerned, the mechanism of O and X-points seems to act as a qualitatively similar way for $(0,7)$ islands in QSH and for the $(0,1)$ island in MH [9]. Indeed, in MH the maximum of the shift $\Delta(m=1, |n|>7)$ is located between the O- and X-points of the $(0, 1)$ island and constitutes the main source of particles [12].

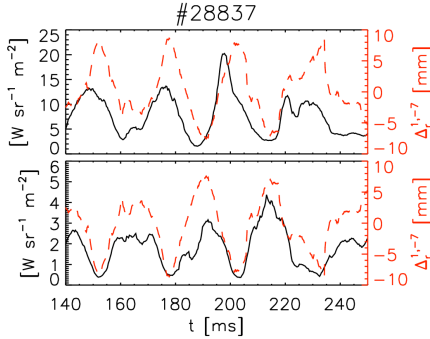


Fig.2: Time behavior of H_α emission for 2 chords (HFS and LFS) compared with corresponding magnetic shift $\Delta_{1,-7}$

source for QSH states as can be deduced by the modulation of H_α emission (see Fig.2). The phase relation between $m=0$ and $m=1$ changes with the poloidal angle: the maximum $\Delta_{1,-7}$

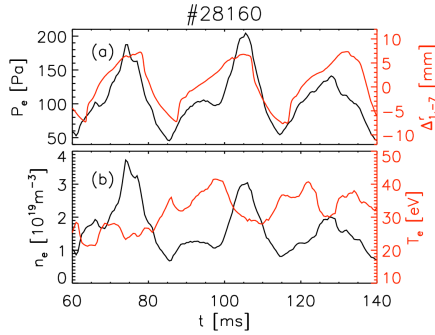


Fig.3: (up) Local time behavior of electron pressure (black) at $r/a=0.97$, compared with the local plasma shift due to the dominant mode (red); (down) time behavior of electron density (black) and temperature (red).

corresponds to the O- and X-points in the top and bottom of the plasma, respectively. In Fig.2 is show the time behavior of H_α emission measurement along two vertical chords (Low- and High-Field Side at the same toroidal position) compared with the corresponding magnetic shift. The H_α maxima coincide with the maximum value of $\Delta_{1,-7}$, both in the HFS and LFS. Regarding the time behavior the two emissions are anti-correlated. The comparison of the two chord emissions gives the hint of helical Plasma Wall Interaction (PWI). The equilibrium between source of particles due to this magnetic shift modulation and a possible sink of particle in the X-points of $(0, 7)$ islands could be at the origin of QSH-MH density limit transition at $n_{c\leq 0.4n_G}$ [9]. This behavior depends also from

the recycling level of the graphite wall: the plasma performance may be improved through wall lithization.

2.2 Edge pressure profile

The time evolution of electron density and temperature in the plasma boundary is measured by the THB diagnostic, which supplies the radial profile in the outmost 30mm (on the equatorial plane LFS) with a time resolution of 3ms. There is a strong dependence of n_e on the shift of the dominant mode $\Delta_{1,-7}$: when the shift is outwards the density presents a local increase of $1\div 2 \cdot 10^{19} \text{m}^{-3}$ (about 100%) with a corresponding decrease of local electron temperature T_e of $5\div 10 \text{eV}$ (about 20%). Thus, the corresponding electron pressure P_e exhibits a good correlation with $\Delta_{1,-7}$: Fig.3 shows an example of the time behavior of P_e compared

with $\Delta_{1,-7}$ (top panel); the time behavior of n_e and T_e is reported in the bottom panel, showing the anti-correlation between the two quantities. In Fig.4 the corresponding radial profiles in two time windows of 3ms characterized by inward and outward magnetic shifts are shown:

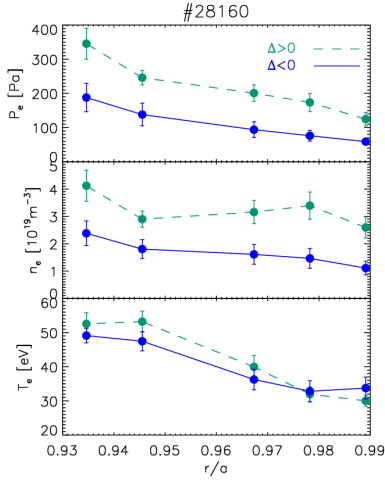


Fig.4: Radial profiles for P_e , n_e , T_e in outward ($\Delta>0$) and inward ($\Delta<0$) local magnetic shift

trend, more evident in the region of negative shift, where the magnetic surface does not touch the wall. For $\Delta_{1,-7}>0$ the experimental points are more scattered, even if a trend is still recognizable: indeed when the magnetic lines intercept the wall close to the diagnostic, the strong local plasma-wall interaction might cause a local increase of the electron density and consequently of the electron pressure. An analogous trend has been observed also for the

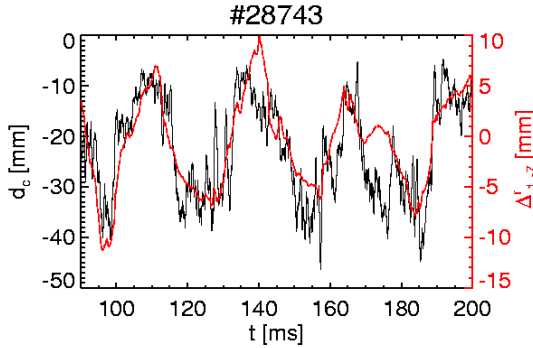


Fig.6: Time modulation (by reflectometer) of radial distance from the wall of layer density of $10^{19}m^{-3}$ which agrees with the local magnetic shift

local shift $\Delta_{1,-7}$, for a plasma discharge of $I_p=1.7MA$, $n/n_G \sim 0.2$, confirming the intrinsic relation between edge density and local magnetic topology.

2.3 Toroidal pattern of floating potential

The boundary of QSH states is also characterized by a modulation of floating potential V_f with the dominant mode $n=-7$. In Fig. 7 the contour plot of the floating potential as a function of time and toroidal angles is shown in the panel (a) as obtained from the toroidally

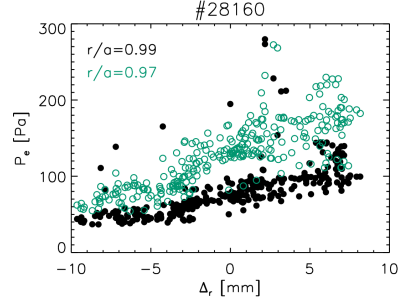


Fig.5: Behavior of P_e with local magnetic shift for two radial positions

electron pressure gradient. Both electron pressure and the corresponding gradient do not depend on the plasma current in the negative shift region, instead a scaling with the current can be observed in the outward magnetic shift regions. Similar results for boundary electron density have been found using the single wavelength microwave reflectometer [13] monitoring the edge density of RFX-mod. This diagnostic system is able to get the radial distance d_c from the first wall of a density layer at $10^{19}m^{-3}$ with a high time resolution ($2\mu s$). In Fig.6 is shown a time modulation of d_c signal with the

local shift $\Delta_{1,-7}$, for a plasma discharge of $I_p=1.7MA$, $n/n_G \sim 0.2$, confirming the intrinsic relation between edge density and local magnetic topology.

distributed array of electrostatic pins pertaining to the ISIS system. The $n=7$ modulation can be clearly recognized and can be linked to the helical deformation induced by the $m=1$ modes shown in panel (b). To simplify the comparison, in panel (c) the floating potential fluctuation and the radial helical deformation are shown as a function of toroidal angle for a fixed time to highlight their spatial correlation.

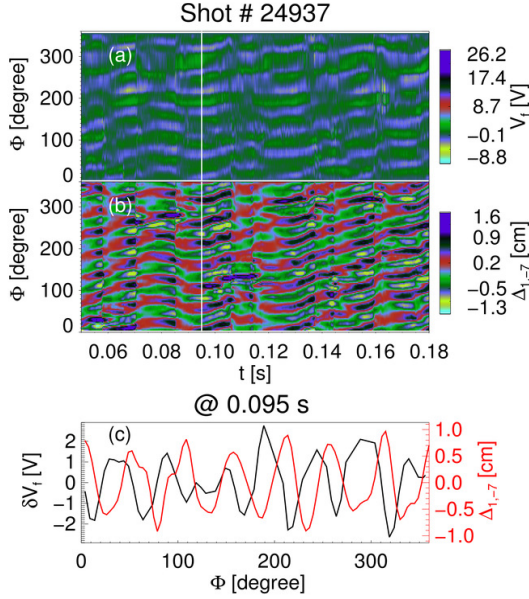


Fig.7: a) contour plot (time-toroidal angle) of V_f b) counter plot of corresponding magnetic shift c) toroidal behavior of V_f fluctuation compared with local magnetic shift for a fixed time.

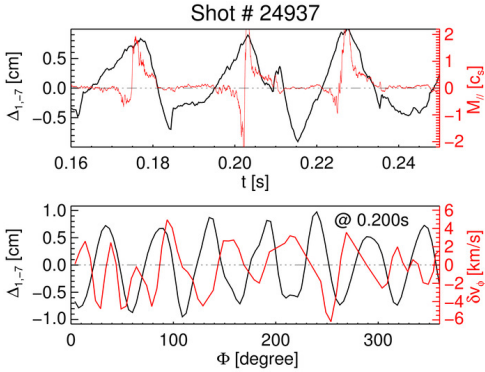


Fig.8: (up) time behavior of $M_{||}$ with local shift; (down) toroidal behavior of flow fluctuations $\Delta_{1,-7}$ compared with local magnetic shift for a fixed time.

In particular the positive value of the plasma shift corresponds to the maximum proximity [14,15]. This interpretation is corroborated by the spatial information obtained through the ISIS system. The toroidal component of the velocity fluctuation is shown as a function of the toroidal angle for a fixed time in the bottom panel of the same Fig.8. The flow fluctuations exhibit a toroidal ripple with the minima corresponding to the maximum values of the plasma shift. The same information has been obtained also through the GPI diagnostic [14]. This experimental result agrees with the behavior of an ambipolar radial electric field which

highlight their spatial correlation. The stronger negative V_f fluctuations correspond to the outwards shift, so that the increased PWI due to the $m=1$ shift produces a local increase of negative V_f as if electrostatic probes mounted at the wall would explore a more internal plasma region [10]. This picture contributes to show the link in the edge of QSH states between the magnetic modes and the kinetic effect: indeed lower negative values of floating potential can be interpreted as an enhancement of electron fluxes collected by the probe, consistent with the observed reduction of electron characteristic length $L_{||}$ in the region of outwards shifts.

2.4 Edge flow behavior in QSH

The flow in the extreme periphery is evaluated using different diagnostics: first of all Gundestrup probe which supplies both the components of Mach number at the wall (toroidal M_{\perp} and poloidal $M_{||}$) [14]. In the QSH states the edge flow presents a modulation with the local shift $\Delta_{1,-7}$. In the top panel of Fig.8 it is shown an example of time behavior of parallel Mach number together with the time evolution of the local magnetic shift at the same toroidal position: around the maximum values of the shift an abrupt variation with a change of the sign of the parallel flow is observed. This behavior has been interpreted in the framework of a helical flow associated to the dominant mode and of the consequent time dependent proximity of the (1,-7) magnetic islands to the diagnostic position.

balances the electron and ion fluxes in a sheath next to the wall [9]. All these information support also the idea of a helical flow surrounding the magnetic island (1,-7) [15]: the role of this flow in QSH sustaining is under investigation.

3. Dynamic of QSH crash events

At high current the QSH states are transiently perturbed by bursts of MHD activity, which presently limit QSH duration and deteriorate the confinement [12]. Moreover, the QSH persistency decreases as a function of n/n_G . The MHD activity perturbing the helical state is toroidally localized and their occurrence seems to be rather randomly distributed in space as

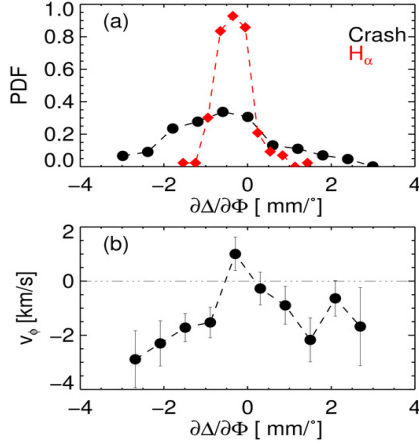


Fig.9: a) PDF of crash events (toroidally random distributed) compared with PDF of H_α emission (at fixed toroidal angle) as function of local shift toroidal derivative; b) Plasma toroidal velocity at crash position as function of local shift toroidal derivative

observed with ISIS diagnostic. After each event the dominant mode amplitude is strongly reduced, although more detailed analysis reveals that it does not vanish completely: these events are partial crashes of helical states and they are the consequence of impulsive magnetic reconnections accompanied by poloidal current sheets moving in the toroidal direction [7, 16]. To study the space relation between the toroidal positions of the crash events and those of (0,7) magnetic islands, the Probability Distribution Function (PDF) of such events has been analyzed as a function of the toroidal derivative of magnetic shift $\Delta_{1,-7}$ around the random toroidal position where the events occur. In other words, we want to locate the time-dependent, intermittent crash events with respect to the (static) topology shown in Fig.1. The PDF is shown in Fig.9a with black dots, revealing the presence of a crash mainly for negative values of $\partial\Delta/\partial\phi$, i.e. in the X-point region of the (0, 7) islands.

A similar analysis has been done for H_α emission and it is shown in the Fig.8a in red: in this case the PDF is computed determining, for a large database, the value

of the derivative of the magnetic shift corresponding to the time occurrence of the maxima of H_α signal in a fixed toroidal angle. The maximum PWI, corresponding to the maximum H_α emission, is observed at a value of $\partial\Delta/\partial\phi$ similar to those obtained for the crash events, this result suggests that the impulsive magnetic reconnections, found in proximity of the X-points of the (0,7) islands, are favoured by a local enhancement of plasma density and associated cooling due to the PWI.

The toroidal velocity of the crash events has been measured with ISIS system and in Fig.9b these values are shown as function of $\partial\Delta/\partial\phi$. A decrease of plasma velocity is observed, with a reversal of the direction corresponding to the maximum probability of reconnection events. This behavior is similar to the dynamic of particle source and accumulation described in [9] for the MH states and could contribute to the crashes limiting the QSH states.

4. Particle in-flux measurements

The described helical PWI that characterizes the plasma boundary during QSH states has also a crucial effect on the in-flux Γ_{in} and in determining the edge transport. An effective technique to mitigate the different PWI observed with the inward and outward magnetic shifts has been found to be wall conditioning by Li pellet injection [17]. The particle in-flux measured by the

H_α emission is shown in Fig.10 as a function of magnetic shift for two discharges (standard and lithized wall at 1.5MA and $n/n_G \sim 0.1$). In standard discharges Γ_{in} is about $10^{21} \text{ m}^{-2} \text{ s}^{-1}$ for inward shift and increases up to $5 \cdot 10^{21} \text{ m}^{-2} \text{ s}^{-1}$ for outward shift. On the other side in Li

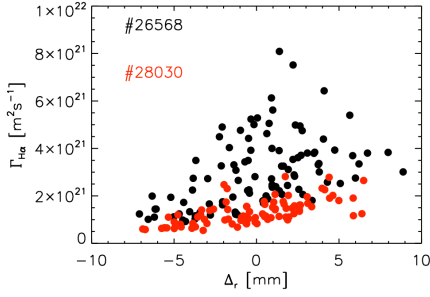


Fig.10 Particle in-flux from H_α emission as function of local magnetic shift for standard and lithized (red) plasma

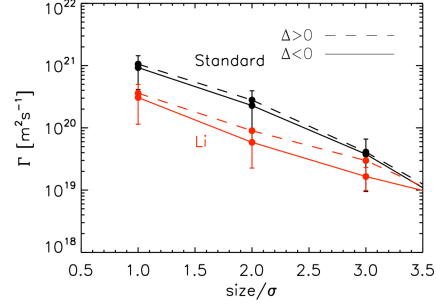


Fig.11: Particle out-flux versus event-amplitude threshold for different local shift in standard and lithized plasma

conditioned discharges Γ_{in} is lower and the discrepancy for the different shifts is about a factor two, highlighting the beneficial effects of Li-conditioning [17] and reducing the coupling between magnetic topology and recycling pattern, which is recognized to be a key ingredient in many density limiting phenomena [18]. The in-flux Γ_{in} has been compared with out-flux Γ_{out} due to the edge blobs evaluated from the THB measurements [4], considering different density fluctuation thresholds. In Fig.11 the average value of Γ_{out} versus event-amplitude thresholds (expressed as a multiplier of rms) is shown in time windows corresponding to different values of the shift $\Delta_{1..7}$; these trends do not present an evident difference between the inward and outward shift, indicating that the particle out-flux due to the blobs does not depend on the shift. Intermittent events detected with the $2\text{-}\sigma$ threshold give an average out-flux of $0.5 \cdot 10^{21} \text{ m}^{-2} \text{ s}^{-1}$ for the standard discharges that corresponds to about 25÷50% of Γ_{in} for inward shift and 5÷10% for outward shift. The Γ_{out} value for the same threshold with wall lithized has been estimated about 1÷5% of Γ_{in} . This means that the Li wall conditioning has also a beneficial effect in decreasing the level of intermittent event of boundary turbulence.

5. QSH persistency and density limit

The maximum duration (persistence) of QSH states has been obtained at high current and low Greewald fraction [12]: contemporary at higher values of n/n_G an increase of the amplitude of the $m=0$ modes is observed [9]. No QSH states are obtained at $n/n_G \geq 0.4$ and this threshold depends on the plasma equilibrium which defines also the distance of the reversal surface from the wall [7]. The QSH states with highest density are obtained, for a given input power, at $q(a) \sim 0.06$. On the contrary, the longest QSH states have been obtained with $q(a) \sim 0.02$ and relatively low density, $n/n_G < 0.2$ and $I_p \geq 1.5 \text{ MA}$. It is interesting to note that there is a competition, for each plasma equilibrium, between the radial displacement $\Delta(m=0)$ due to the $m=0$ modes and the distance of reversal from the wall ($a-r_{rev}$). The ratio of these two quantities, can be considered as a ‘‘Chirikov wall’’ C_w parameter [9] and indicates whether the $m=0$ islands overlap ($C_w > 1$) the first wall or not ($C_w < 1$). The threshold of C_w in the RFP has an analog in the Tokamak, namely the critical distance of the SOL to the inner wall [19]. From magnetic measurements it is observed that at shallow reversal the $C_w = 1$ value has been reached at lower n/n_G : in this case the $m=0$ islands intercept the wall at lower normalized density. The $m=0$ islands overlapping the wall cause a local increase of electron diffusion and of $m=0$ modes: when the harmonic $n=1$ increases and is able to modulate the $(0, 7)$ mode, back-transitions from QSH to MH states are observed.

6. Conclusions

In this paper we have described in detail the boundary RFP plasma in the helical state (QSH). In this state the edge plasma is strongly influenced by the helical deformation (ripple) induced by the dominant mode, $\Delta_{1,-7}$. In the regions where this ripple points inwards, both electron pressure and the corresponding gradient do not depend on the plasma current; on the contrary, a scaling of pressure with the current and consequently with the input power can be observed in the regions where the ripple points outwards. Therefore, the behavior of the boundary region with negative values $\Delta_{1,-7} < 0$ seems to be rather independent of the core plasma and it is influenced mainly by local processes and first wall conditioning. Instead, the boundary region with $\Delta_{1,-7} > 0$ is characterized by an enhanced PWI with local density increase and plasma cooling, more negative floating potential and an increased plasma toroidal flow. These phenomena are a consequence of a stronger correlation with core processes.

It is worth underlining that impulsive magnetic reconnections which limit QSH duration and performances are favored by this local enhancement of plasma density and corresponding plasma cooling. Therefore, QSH persistence and the critical density which determines its disappearance seem to be closely linked to the boundary conditions.

Finally, an indication of an helical flow associated to the dominant mode has been shown: further investigation are now mandatory, in order to establish the role of this flow in the formation of improved confinement regimes, together with the comprehension of its role in the determination of dynamo electric field which sustains the helical equilibrium.

References

- [1] G. Spizzo, et al. *Physical Review Letters*, **96** (2006) 025001
- [2] R. Paccagnella, et al *Physical Review Letters* **97** (2006) 075001; L. Marrelli, et al. *Plasma Phys. and Control. Fusion*, **49** (2007) B359
- [3] M. E. Puiatti, et al. *Plasma Phys. and Control. Fusion*, **51** (2009)124031
- [4] M. Agostini et al. *Plasma Phys. and Control. Fusion* **51** (2009) 105003;
M. Agostini et al. “*Optical measurements for Turbulence Characterization in RFX-mod edge*” accepted for publication in Rev. Sci. Instrument
- [5] G. Serianni, et al. *Rev. Sci. Instrum.*, **74** (2003) 1558
- [6] P. Zanca et al. *Plasma Phys. and Control. Fusion*, **46** (2004) 1115
- [7] S. Cappello and D. Biskamp. *Nucl. Fusion*, **36** (1996) 571.
- [8] P. Scarin, et al. *Journal of Nuclear Materials* **390** (2009) 444
- [9] G. Spizzo, et al. *Plasma Phys. and Control. Fusion*, **52** (2010) 095011
- [10] E. Martines, et al. *Nuclear Fusion*, **50** (2010) 035014
- [11] R. B. White and M. S. Chance. *Physics of Fluids*, **27** (1984) 2455–2467
- [12] M. E. Puiatti et al. *Nuclear Fusion* **49** (2009) 045012
- [13] G. De Masi et al. “*Ultrafast reflectometry on the RFX-mod device*” 37th EPS Conf. on Pl. Phys. (Dublin 2010) <http://ocs.ciemat.es/EPS2010PAP/pdf/P5.104.pdf>
- [14] M. Spolaore et al. “*Parallel and perpendicular flows in the RFX-mod edge region*” accepted for publication in Journal Nucl. Mater.
- [15] D. Bonfiglio et al. “*Role of flow in the formation of helical states in RFX-mod*” 37th EPS Conf. on Pl. Phys. (Dublin 2010) <http://ocs.ciemat.es/EPS2010PAP/pdf/O2.101.pdf>
- [16] Zuin M. et al *Plasma Phys. Control. Fusion* **51** (2009) 035012
- [17] S. Dal Bello et al. “*Lithisation effects on density control and plasma performance in RFX-mod experiment*” , this conference.
- [18] Y. Liang et al. *Phys. Rev. Lett.*, **94** (2005) 105003
- [19] P. C. de Vries, J. Rapp, F. C. Schüller, and M. Z. Tokar’, *Phys. Rev. Lett.*, **80** (1998) 3519